Shape isomers and clusterization in the ^{28}Si nucleus

J. Darai
Department of Experimental Physics, University of Debrecen, Debrecen, Pf. 105, Hungary 4010

J. Cseh
Institute of Nuclear Research, Hungarian Academy of Sciences, Debrecen, Pf. 51, Hungary 4001

D. G. Jenkins
Department of Physics, University of York, Heslington, York YO10 5DD, United Kingdom
(Received 13 September 2012; published 10 December 2012)

The shape isomers of the ^{28}Si nucleus are derived from Nilsson model calculations combined with quasidynamical SU(3) symmetry considerations, and their possible binary clusterizations are determined. The results are compared with those of other calculations. Concerning the superdeformed state our finding gives support to the new candidate suggested by Jenkins *et al.* [Phys. Rev. C **86**, 064308 (2012)].

DOI: 10.1103/PhysRevC.86.064309 PACS number(s): 21.10.Re, 21.60.Cs, 21.60.Fw, 21.60.Gx

I. INTRODUCTION

The shape isomers of light nuclei attract much attention from different structure studies, such as shell model, mean-field, cluster models; and provide a close connection to nuclear reactions as well. Superdeformed bands in ^{36}Ar and ^{40}Ca have been well-established through γ-ray spectroscopy [1]. Well-developed rotational bands connected by strong $E2$ transitions are identified in both nuclei. In addition, candidate hyperdeformed states have been suggested from reaction studies [2] but here the connecting electromagnetic transitions are missing which would be the evidence required to clearly demonstrate the associated band structure.

There has been considerable theoretical effort, recently, in considering superdeformed and other highly deformed configurations in ^{28}Si. An AMD study by Taniguchi *et al.* [3] delineates an SD band in ^{28}Si with a moment of inertia of $\approx 6\ \hbar^2$/MeV. Its structure is dominated by $^{24}\mathrm{Mg}+\alpha$ and $^{12}\mathrm{C}+{}^{16}\mathrm{O}$ clustering. Another recent calculation in terms of the macroscopic-microscopic model [4] also predicts an SD band with strong $^{12}\mathrm{C}+{}^{16}\mathrm{O}$ clustering.

From the experimental side, there are a set of states in ^{28}Si identified in the $^{12}\mathrm{C}(^{20}\mathrm{Ne},\alpha)\,^{28}\mathrm{Si}$ reaction which have been attributed to the superdeformed band by Kubono *et al.* [5]. This sequence does not, however, have the smooth characteristics expected for such a band.

Jenkins *et al.* (preceding paper) have reviewed the available experimental data, and extended them with new γ transitions [6]. As a result they propose a new candidate for the SD band. In particular a 6^+ state was identified by Brenneisen *et al.* [7] at 12.86 MeV, which is populated in (α,γ) reaction, but not in (p,γ). In a recent Gammasphere measurement the $^{12}\mathrm{C}(^{20}\mathrm{Ne},\alpha)\,^{28}\mathrm{Si}$ reaction was studied [6]. Double and triple γ coincidences were measured, and nearly all states below 10 MeV have been located, as well as essentially all known γ-decaying high-spin ($J > 4$) states. This work confirms the location and the decay branching of the candidate state by Brennenstein *et al.* As a result the new SD candidate band has states with 2^+, 4^+, and 6^+ spin-parities. Their γ decay is strongly retarded to the oblate ground state band, and enhanced to the prolate band.

Inspired by this exciting situation with open questions on the SD state, we present here an independent theoretical analysis of highly deformed structures in ^{28}Si. In particular we perform a Nilsson calculation, combined with quasi-dynamical U(3) considerations, and determine the allowed binary clusterization of the shape isomers. Our result on the SD state supports the new candidate state proposed by Jenkins *et al.* [6].

II. SHAPE ISOMERS

In our approach the symmetry considerations play an essential role, both in the determination of the shape isomers, and in finding their possible clusterizations.

We obtain the shape isomers from a self-consistent calculation concerning the quadrupole deformation. In doing so we apply the quasidynamical U(3) symmetry [8]. This concept is a generalization of the real U(3) symmetry, known to be approximately valid for light nuclei [9]. The quasidynamical symmetry is more general than the real U(3) symmetry, as the Hamiltonian breaks the symmetry in such a way that the U(3) quantum numbers are not valid for its eigenvectors. In other words, neither the operator is symmetric [i.e., it is not a U(3) scalar], nor its eigenvectors (i.e., they do not transform according to a single irreducible representation) [10]. Yet, the symmetry remains in some form. An asymptotic Nilsson state serves as an intrinsic state for the quasidynamical SU(3) representation. The effective quantum numbers are then determined by the Nilsson states in the regime of large deformation [11]. When the deformation is insufficiently large, we expand the Nilsson states in the asymptotic basis, and calculate the effective quantum numbers based on this expansion [12].

The SU(3) quantum numbers uniquely determine the quadrupole shape of the nucleus [13], and so can be used to determine the properties of shape isomers, by carrying out

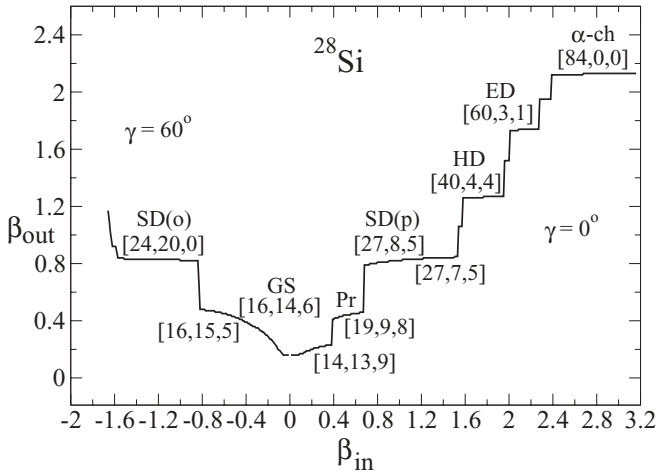

FIG. 1. Quadrupole deformation of ^{28}Si nucleus from the Nilsson model using effective U(3) quantum numbers. The horizontal axis shows the β_{in} input parameter, and the vertical axis indicates the absolute value of β_{out}. The left-hand side corresponds to $\gamma_{in} = 60^\circ$ while the right hand side represents $\gamma_{in} = 0^\circ$.

a self-consistent calculation with respect to the quadrupole shape of nucleus [14,15]. In practice, this means the continuous variation of the quadrupole deformation (β_{in}, γ_{in}), as an input for the Nilsson-model, and determining the effective U(3) quantum numbers or, from them, the corresponding β_{out}, γ_{out} quadrupole deformation. This method for describing shape isomers is a useful alternative to the standard energy-minimum calculation and has been shown to be effective for a range of light nuclei [14–17].

The result of the Nilsson model + quasidynamical SU(3) calculation is shown in Fig. 1 for $\gamma_{in} = 60^\circ$ and $\gamma_{in} = 0^\circ$. In this figure, the horizontal plateaus rather than the minima correspond to stable shapes. Similar calculations have been performed for intermediate values of γ in steps of 5°; the results for $\gamma_{in} \leqslant 30^\circ$ are broadly similar to those for $\gamma_{in} = 0^\circ$, and calculations for $\gamma_{in} > 30^\circ$ are similar to those for $\gamma_{in} = 60^\circ$. The properties of the shape isomers identified in the calculations are given in Table I, along with close-lying configurations in the simple harmonic oscillator (HO) shell model. The moment of inertia in the last column of the table (in $\hbar^2$/MeV units) is calculated for rigid ellipsoids with the shape determined by the U(3) symmetries. For triaxial shapes, the moment of inertia is given for each major axis in turn and for cylindrically symmetric shapes only the relevant value is shown.

The calculations reproduce the well-established competition between oblate and prolate minima at low energy (see Fig. 1). The next shape isomer on the prolate side is a very pronounced plateau at $4\hbar\omega$ excitation, although with some fluctuation of the effective symmetry (or quadrupole shape). This state corresponds to a prolate superdeformed shape [SD(p)]. On the oblate side, there is an $8\hbar\omega$ shape, which is also stable with even less fluctuation. This is labeled as oblate superdeformed state [SD(o)], though the ratio of the long and short axes is somewhat greater than 2. Both the prolate and the oblate SD states have an associated triaxiality close to the expected values of $\gamma = 0^\circ$ and $\gamma = 60^\circ$, respectively. The next prolate state appears at $12\hbar\omega$ excitation, and is cylindrically symmetric. The effective U(3) quantum numbers coincide with the ones expected from the simple HO shell model, and the ratio of the major axes is 3:1:1, corresponding to a hyperdeformed (HD) state. At even larger prolate deformation, an extremely deformed (ED) state is identified. Finally, the linear α-chain (α-ch) emerges with $48\hbar\omega$ excitation quanta.

TABLE I. Shape isomers in the ^{28}Si nucleus from the Nilsson model + quasidynamical SU(3) calculation. 'e' stands for effective U(3) quantum numbers, 'h' indicates the states corresponding to simple harmonic oscillator configurations. 'e*' refers to a triaxial solution which does not appear in Fig. 1; 'a' denotes the result of the α-cluster calculation [18], (p) and (o) mean prolate and oblate, respectively. The triaxiality, γ, is given in degrees. The penultimate column indicates the axis ratio, while the final column presents the moment of inertia (in units of $\hbar^2$/MeV).

State	Model	$\hbar\omega$	U(3)	β_2	γ	a:b:c	$\mathcal{J}$
	e(p)	−1	[13,13,9]	0.17	60	1.2:1.2:1	3.4
GS	e(o)	0	[16,15,5]	0.44	55	1.6:1.5:1	4.8
							3.5
							3.3
	h	0	[16,16,4]	0.50	60	1.7:1.7:1	3.4
Pr	e	0	[19,9,8]	0.44	5	1.5:1:1	4.4
							4.3
							2.8
	h	0	[20,8,8]	0.50	0	1.5:1:1	4.5
SD(p)	e	4	[27,8,5]	0.81	7	2.2:1.1:1	5.8
							5.5
							2.3
	h	4	[28,8,4]	0.88	9	2.3:1.2:1	6.1
							5.7
							2.2
SD(o)	e	8	[24,20,0]	0.84	51	2.7:2.4:1	6.7
							4.2
							3.5
	h	8	[24,20,0]	0.84	51	2.7:2.4:1	6.7
							4.2
							3.5
Tri	e*	12	[35,8,5]	1.03	5	2.6:1.2:1	6.8
							6.6
							2.0
	h	12	[36,8,4]	1.08	7	2.8:1.2:1	7.2
							6.9
							2.0
	a	12	[36,12,0]	1.14	19	3.6:2.6:1	8.2
							6.9
							2.2
HD	e	12	[40,4,4]	1.29	0	3:1:1	8.6
	h	12	[40,4,4]	1.29	0	3:1:1	8.6
ED	e	28	[60,3,1]	1.76	2	4.9:1.1:1	14.5
							14.3
							1.3
	h	28	[60,4,0]	1.76	3	5.3:1.3:1	14.6
							14.3
							1.3
α-ch	e	48	[84,0,0]	2.14	0	7:1:1	24.3
	h	48	[84,0,0]	2.14	0	7:1:1	24.3

The triaxial state (Tri) was found in the calculations around $\gamma = 20^\circ$, as the only further candidate for the shape isomers in addition to those shown in Fig. 1.

It is appropriate to compare the present calculations with earlier determinations of shape isomers using Nilsson model potential energy surfaces [19], and the Bloch-Brink α-cluster model [18,20,21]. Leander and Larsson list five shape isomers [19]; three of them practically identical with the GS, Pr, and HD states in the present work. They do not, however, identify a state corresponding to the prolate superdeformed state, but do find states fairly similar to the $8\hbar\omega$ excitation (oblate superdeformed) and ED states [19]. α-cluster calculations by Rae *et al.* [18,20,21] resulted in eight shape isomers, as in the present work. Since Ref. [21] gives the corresponding shell model configurations, a detailed comparison with the present work is possible, leading to the conclusion that the three-dimensional cluster states in [21] are completely identical with our GS, Pr, SD(p), and HD states. In [18] three states were found with two-dimensional cluster configurations. The first is identical with our SD(o) state, the second corresponds approximately to the Tri state, while the third one is also a triaxial state, which is not seen in Fig. 1. The alpha-chain state of [20] is identical to our one. Thus the comparison between the α-cluster calculations and the present work reveals very strong similarities: eight shape isomers in both works, of which seven show a one-to-one correspondence.

As mentioned before, the present method of the determination of the shape isomers is based on the self-consistency requirement with respect to the quadrupole shape, and not on the calculation of the energy surface. Therefore, no direct result is obtained for the excitation energies of the states in Table I. Nevertheless, it is informative to recall the energy values obtained for these states from other works. Especially useful is the comparison with the α-cluster model, due to the fact, that six of the shape isomers obtained here are completely identical [has the same U(3) symmetry] with the corresponding states from the Bloch-Brink model [18,20,21], and the seventh one has a close similarity. Their excitation energies are as follows (in MeV): Pr: -2.7, SD(p): 10.3, SD(o): 29.9, Tri: 35.0, HD: 23.8, α-ch: 60.2. Note, that in the α-cluster model study the oblate structure were found to be systematically underbound with respect to the prolate structures [21]. As for the superdeformed state, the more recent calculations [3,4] and the new experimental candidate band [6] also suggest a similar energy.

III. CLUSTER CONFIGURATIONS

The building up of an atomic nucleus from smaller clusters is governed by two basic physical laws: the energy-minimum principle, and the Pauli exclusion principle. These two considerations may prefer the same cluster configuration, but this is not necessarily the case. We consider a cluster configuration as a likely one, if it is Pauli allowed, and preferred by the energetics. In determining the energetic preference we apply the binding energy arguments of [22]. The exclusion principle is incorporated by using selection rules, based on the microscopic structure: Harvey's prescription [23], and the U(3) selection rule (for a recent review and applications see [14,15,17,24]).

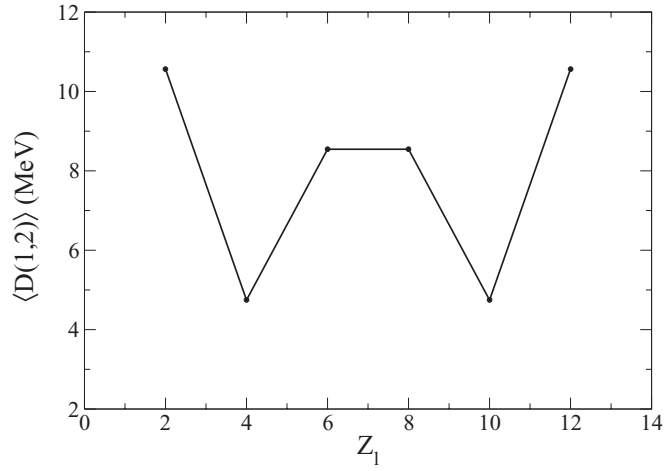

FIG. 2. Energetic stability of binary even-even cluster configurations in ^{28}Si. Z_1 stands for the charge of the lighter cluster.

A. Energetic preference

The criterion for maximal stability [22] corresponds to maximising the summed differences of the measured binding energies and the corresponding liquid drop values:

$$D(1,2) = [B(1) - B_L(1)] + [B(2) - B_L(2)], \qquad (1)$$

where $B(i)$ is the experimental binding energy of the ith cluster [25], while $B_L(i)$ stands for the liquid drop value. In the generalised version of the method, as we apply it here, a further condition is also taken into account, known as the dipole constraint [22]. It is based on the observation that electric dipole transitions are very weak, therefore, the decomposition $A_T \to A_1 + A_2$ (here T stands for total) is expected to be close to satisfying the constraint:

$$\frac{Z_1}{A_1} \approx \frac{Z_T}{A_T} \approx \frac{Z_2}{A_2}. \qquad (2)$$

In this approach, the α-like cluster configurations turn out to be more stable than the other possibilities. The most preferred clusterization is that of ^{4}He + ^{24}Mg, followed by the ^{12}C + ^{16}O (see Fig. 2).

B. Structural selection

For a binary cluster configuration, the U(3) selection rule reads

$$[n_1, n_2, n_3] = \left[n_1^{(1)}, n_2^{(1)}, n_3^{(1)}\right] \otimes \left[n_1^{(2)}, n_2^{(2)}, n_3^{(2)}\right] \otimes [n^{(R)}, 0, 0], \qquad (3)$$

where $[n_1, n_2, n_3]$ is the set of U(3) quantum numbers of the parent nucleus, the superscript (i) stands for the ith cluster, and (R) indicates relative motion.

Characterizing the nuclei (clusters) by their U(3) symmetry means that they are supposed to be in their ground intrinsic states, but collective excitations (belonging to the same irreducible representation) are incorporated. The clusters have deformation (prolate, oblate, triaxial) like real nuclei, and their relative orientation is not restricted in any way. The U(3) selection rule, which deals with the space symmetry of the

states, is always accompanied by a similar $U^{ST}(4)$ [17,26] selection rule for the spin-isospin degrees of freedom.

In addition to the U(3) selection rule, there is another simple rule, which is also based on the microscopic picture, yet is easy to apply systematically—this is Harvey's prescription [23]. This method also applies the harmonic oscillator basis, thus there is a considerable similarity between the selection rule and this prescription. However, they are not identical, rather they are complementer to each other in a sense. Therefore, they should be applied in a combined way [17].

When the real U(3) symmetry is not valid anymore, then the effective U(3) can still provide us with effective (or average) U(3) quantum numbers, and based on that a selection rule can be formulated. Due to the average nature of these quantum numbers, however, the effect of the selection rule is different from that of the real U(3) selection rule. It gives information on the matching, or mismatching of the average nucleon distributions in the cluster configuration and in the shell-model state. Therefore, it acts like a self-consistency check of the quadrupole deformation and the cluster configuration. The fact that for light nuclei the quasidynamical and real U(3) coincide [12] provides a straightforward way to extend the simple selection rule considerations.

When a given cluster configuration is forbidden, we can characterize its forbiddenness quantitatively in the following way [27]. The distance between a U(3) reaction channel and the irreducible representation (irrep) of the parent nucleus is defined as $\min(\sqrt{(\Delta n_1)^2+(\Delta n_2)^2+(\Delta n_3)^2})$, where $\Delta n_i = |n_i - n^c_{i,k}|$. Here n_i refers to the U(3) representation of the parent nucleus, while $n^c_{i,k}$ stands for the U(3) representation of channel c, obtained from the right-hand side of Eq. (3), with the k index distinguishing the different product representations. Based on this quantity we determine, for reasons of convenience, the reciprocal forbiddenness, S in such a way, that $0 \leqslant S \leqslant 1$:

$$S = \frac{1}{1+\min(\sqrt{(\Delta n_1)^2+(\Delta n_2)^2+(\Delta n_3)^2})}. \qquad (4)$$

Then $S \approx 0$, and $S \approx 1$ correspond to completely forbidden and completely allowed cluster configurations, respectively.

Figure 3 shows the reciprocal forbiddenness for the shape isomers found in Table I. The SD(o), ED, and α-ch states do not allow any binary cluster configurations in which the clusters are in their intrinsic ground states. The GS allows those for which the lighter cluster is in either ^{4}He and ^{8}Be. The HD state can be built up only from ^{20}Ne and ^{8}Be (both of them are strongly deformed prolate), in a pole-to-pole configuration, while the Pr, SD(p), and Tri states allow several cluster configurations. For the latter one only the effective U(3) symmetry and the close-lying simple harmonic oscillator configuration lead to clusterization, while the one from the α-cluster model does not.

A few remarks seem to be proper here on the association between the shape isomers, cluster configurations, and the resonance spectra of light heavy-ion reactions. In the superdeformed state both the present work, as well as other recent calculations [3,4] predict important contribution from the ^{24}Mg + ^{4}He and ^{16}O + ^{12}C cluster configurations. This

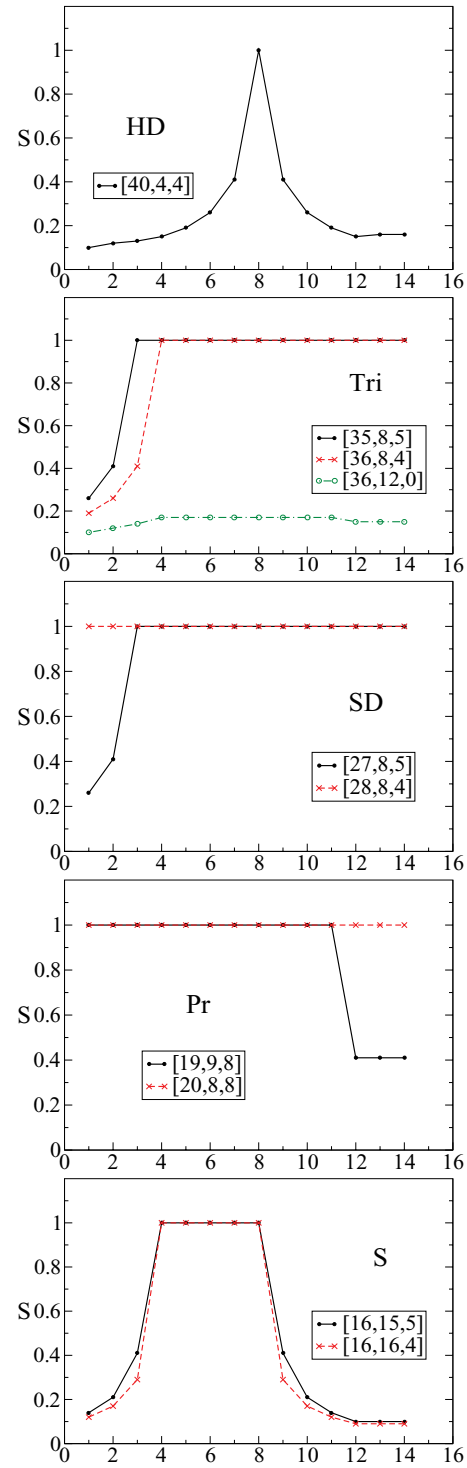

FIG. 3. (Color online) Reciprocal forbiddenness as a function of the mass number of the lighter cluster for the shape isomers in ^{28}Si. The lines are just to guide the eye.

is also in line with the conclusion of the new experimental study of [6]. A rich resonance-spectrum is known both from the ^{24}Mg + ^{4}He reactions in the region of E = 10–15 MeV (see, e.g., [6,7,28,29], and references therein) and from the ^{16}O + ^{12}C collision at E = 20–45 MeV ([30], and references

therein). The $^{24}Mg + ^{4}He$ resonances are around the recently proposed candidate of the SD state [6], and it is interesting to note that their detailed spectrum can be described together with the low-lying bands of the ^{28}Si [31]. The $^{16}O + ^{12}C$ resonances are in a higher-lying region. In [21] they are associated to the hyperdeformed state, but the present considerations show that this cluster configuration (with intrinsic ground states, as prepared by the collision experiments) are forbidden in the HD state. It is more probable that they are located in the local minima corresponding to the superdeformed [SD(p): the very low-energy part] and mainly to the triaxial (Tri) shape. In [32] the detailed spectra of the $^{24}Mg + ^{4}He$ and $^{16}O + ^{12}C$ cluster configurations were described in a unified way in terms of the multichannel dynamical symmetry of the semimicroscopic algebraic cluster model. A renewed study of that kind would be interesting in light of the recent developments on the shape isomers.

IV. CONCLUSIONS

We have analyzed the shape isomers of the ^{28}Si nucleus, and their possible binary cluster configurations. The deformation of the states were determined from self-consistent Nilsson model calculations combined with quasidynamical SU(3) considerations. We have found eight shape isomers ranging from the ground state up to a linear α-chain configuration. Five of them were seen previously in energy calculations of the Nilsson model [19]. Even better agreement is recognised with Brink-model results [18,20,21]. These studies gave also eight shape isomers, and seven of them are in a one-to-one correspondence with our results.

We have studied systematically the allowed binary cluster configurations of the shape isomers. In doing so the clusters were considered to have deformations, like the ground states of the corresponding nuclei, and no constraint was applied for their relative orientation. The α-like clusterizations proved to be energetically favoured. The hyperdeformed state allows only a single binary clusterization (of intrinsic ground state clusters): $^{20}Ne + ^{8}Be$, the ground state can have core $+ \alpha$, as well as core $+ ^{8}Be$. The prolate and the superdeformed state allow several clusterizations. For the SD(p) state, which is the focus of the present work, we find that the $^{4}He + ^{24}Mg$, and the $^{12}C + ^{16}O$ cluster configurations are the most probable, taking account of both the selection rules and energetic preference. This finding is in line with the recent AMD [3] and macroscopic-microscopic calculations [4], as well as with the new experimental results [6]. Its predicted moment-of-inertia is near-identical to that of the AMD calculation, and showed by the experiment, thus it gives support to the new candidate for the SD state [6].

ACKNOWLEDGMENTS

This work was supported by the OTKA (Grant No. K72357), by the TAMOP (4.2.1./B-09/KONV-2010-0007/IK/IT), and by the MTA-JSPS bilateral project (No. 119). Inspiring discussions with T. Ichikawa, Y. Kanada-En'yo, and Y. Taniguchi are gratefully acknowledged.

[1] C. E. Svensson *et al.*, Phys. Rev. Lett. **85**, 2693 (2000); E. Ideguchi *et al.*, *ibid.* **87**, 222501 (2001).
[2] W. Sciani *et al.*, Phys. Rev. C **80**, 034319 (2009); A. Lepine-Szily *et al.* (unpublished).
[3] Y. Taniguchi, Y. Kanada-En'yo, and M. Kimura, Phys. Rev. C **80**, 044316 (2009).
[4] T. Ichikawa, Y. Kanada-En'yo, and P. Moller, Phys. Rev. C **83**, 054319 (2011).
[5] S. Kubono *et al.*, Nucl. Phys. A **457**, 461 (1986).
[6] D. G. Jenkins *et al.*, Phys. Rev. C **86**, 064308 (2012).
[7] J. Brenneisen *et al.*, Z. Phys. A **352**, 149 (1995); **352**, 279 (1995); **352**, 403 (1995).
[8] P. Rochford and D. J. Rowe, Phys. Lett. B **210**, 5 (1988); D. J. Rowe, P. Rochford, and J. Repka, J. Math. Phys. **29**, 572 (1988).
[9] J. P. Elliott, Proc. Roy. Soc. A **245**, 128 (1958); **245**, 562 (1958).
[10] J. Cseh, *Proceedings of the IV International Symposium on Quantum Theory and Symmetries (Varna)* (Heron Press, Sofia, 2006), p. 918.
[11] M. Jarrio, J. L. Wood, and D. J. Rowe, Nucl. Phys. A **528**, 409 (1991).
[12] P. O. Hess, A. Algora, M. Hunyadi, and J. Cseh, Eur. Phys. J. A **15**, 449 (2002).
[13] D. J. Rowe, Rep. Prog. Phys. **48**, 1419 (1985).
[14] J. Cseh, J. Darai, W. Sciani, Y. Otani, A. Lepine-Szily, E. A. Benjamim, L. C. Chamon, and R. L. Filho, Phys. Rev. C **80**, 034320 (2009).
[15] J. Darai, J. Cseh, N. V. Antonenko, G. Royer, A. Algora, P. O. Hess, R. V. Jolos, and W. Scheid, Phys. Rev. C **84**, 024302 (2011).
[16] J. Cseh, J. Darai, A. Algora, H. Yepez-Martinez, and P. O. Hess, Rev. Mex. Fis. S **54**, 30 (2008).
[17] J. Cseh and J. Darai, AIP Conf. Proc. **1098**, 225 (2009), and references therein.
[18] J. Zhang and W. D. M. Rae, Nucl. Phys. A **564**, 252 (1993).
[19] G. Leander and S. E. Larsson, Nucl. Phys. A **339**, 93 (1975).
[20] A. C. Merchant and W. D. M. Rae, Nucl. Phys. A **549**, 431 (1992).
[21] J. Zhang, W. D. M. Rae, and A. C. Merchant, Nucl. Phys. A **575**, 61 (1994).
[22] B. Buck, A. C. Merchant, and S. M. Perez, Few-Body Systems **29**, 53 (2000); B. Buck, A. C. Merchant, M. J. Horner, and S. M. Perez, Phys. Rev. C **61**, 024314 (2000).
[23] M. Harvey, Proceedings of the 2nd International Conference on Clustering Phenomena in Nuclei, College Park, MD, USDERA report ORO-4856-26, p. 549 (1975).
[24] J. Cseh, A. Algora, J. Darai, and P. O. Hess, Phys. Rev. C **70**, 034311 (2004).
[25] G. Audi, A. H. Wapstra, and C. Thibault, Nucl. Phys. A **729**, 337 (2003).
[26] E. P. Wigner, Phys. Rev. **51**, 106 (1937).

[27] A. Algora and J. Cseh, J. Phys. G: Nucl. Part. Phys. **22**, L39 (1996).
[28] J. Cseh, E. Koltay, Z. Máté, E. Somorjai, and L. Zolnai, Nucl. Phys. A **385**, 43 (1982).
[29] P. M. Endt, Nucl. Phys. A **521**, 1 (1990).
[30] U. Abbondano, Trieste Report No. INFN/BE-91/11, 1991.
[31] J. Cseh, Phys. Lett. B **281**, 173 (1992).
[32] J. Cseh, Phys. Rev. C **50**, 2240 (1994).